Tribology Letters (2019) 67:103
https://doi.org/10.1007/s11249-019-1216-1

ORIGINAL PAPER

Vibration and Noise Behaviors During Stick–Slip Friction

Dong Conglin[1,2,3] · Mo Jiliang[4] · Yuan Chengqing[1,3] · Bai Xiuqin[1,3] · Yu Tian[2]

Received: 9 April 2019 / Accepted: 20 August 2019 / Published online: 4 September 2019

Abstract
Frictional vibration and noise usually cause machining error and noise pollution. Stick–slip plays an important role in generating frictional vibration and noise. This study characterized frictional vibration and noise during the stick–slip of a Si_3N_4 ceramic/metal friction by using an acoustic emission method. Experimental results showed that frictional vibration and noise mostly occurred during the slip process. The impacts of the rough peaks between metal disk and ceramic ball during sliding induced the vibration to irradiate noises. The superposition among the frictional vibrations caused the multiplication of vibrational frequency. The major vibrational frequency slowly shifted to a higher frequency as the increase in sliding speed. The vibrational accelerations and their major vibrational frequency increased with the increase in the external load. The knowledge gained herein provides a more comprehensive understanding of stick–slip friction, frictional vibration, and noise, and offers a guidance for controlling or minimizing stick–slip, frictional vibration, and noise.

Keywords Frictional vibration · Frictional noise · Stick–slip · Acoustic emission

1 Introduction

Friction usually causes wear and vibration at the contact interface. Frictional vibration is a phenomenon that has been an important concern for many centuries throughout a broad interesting area from daily activities, general machines, various manufacturing techniques, automobiles, water and underwater vehicles, and aerospace applications [1–5]. This phenomenon generally causes machining error and noise pollution. Several comprehensive reviews [1–7] have reported research on frictional vibration and noise of over 70-year studies. Numerous studies have been conducted to reveal the possible generating mechanisms of frictional noise. Theories have been proposed in several classes, such as stick–slip, hammering excitation, and mode coupling of structures [8–13]. In addition, time delay [14], moving load [15], and positive friction–velocity characteristics [16] have also been proposed as possible causes of friction noise. These mechanisms are useful for a thorough understanding of the origin of friction noise. However, analyzing the vibration and noise by in situ measurement is difficult. Frictional vibration and noise are usually caused by multiple physical processes, but an effective decoupling method for resolving different influence factors from the coupling process remains lacking [17–20].

Stick–slip, a key phenomenon in friction, has been extensively studied to explore the friction mechanism and guide various applications [21–24]. Factors, such as velocity, load, and temperature, can significantly affect the energy accumulation in the stick process and the energy releasing in the slipping process, thereby causing the tribological system to be unstable instantaneously and inducing vibration and noise [25–28]. Numerous experimental studies have been conducted to study frictional vibration noise during the stick–slip motion [29–31]. Popp found that the stick–slip motion can induce self-sustained oscillations to result in a robust limit cycle and eventually radiate frictional vibration and noise [32]. Charles found that friction between rubbing pairs produce stick–slip behavior at intermediate shear rates

✉ Yu Tian
tianyu@mail.tsinghua.edu.cn

1 Reliability Engineering Institute, National Engineering Research Center for Water Transport Safety, Wuhan University of Technology, Wuhan 430063, People's Republic of China

2 State Key Laboratory of Tribology, Tsinghua University, Beijing 100084, China

3 Key Laboratory of Marine Power Engineering & Technology (Ministry of Transport), Wuhan University of Technology, Wuhan 430063, People's Republic of China

4 Tribology Research Institute, Southwest Jiaotong University, Chengdu 610031, People's Republic of China

and eventually cause frictional noise, even if the material is strengthened at large rates [33]. Johnson reported that acoustic emission (AE) and shear microfailure (microslip) phenomena exhibit an exponential increase in occurrence rate during the stick–slip process, and caused frictional noise increases evidently [34].

However, few studies have been conducted on the frictional noise during stick–slip processes. The present study investigated the frictional vibration and noise using the AE method and examined the shearing or impacting signals between rubbing pairs to disclose the mechanisms of frictional vibration. This study aimed to understand the mechanisms of frictional vibration and noise behaviors comprehensively and provide guidance for controlling and minimizing frictional vibration and noise behaviors.

2 Methods and Experiments

2.1 Materials and Test Setup

Si_3N_4 ceramic balls with a diameter of 7 mm were selected as test parts. A 304 stainless steel was converted into disk specimens as the counterpart with a diameter of 100 mm, a height of 10 mm, and a mean surface roughness Sa of 0.2 ± 0.05 μm.

All friction tests were performed on a commercial ball-on-disk friction testing machine (UMT-3 tribotester, Center for Tribology, Inc.), as illustrated in Fig. 1. The upper Si_3N_4 ceramic ball specimen was brought into contact with the lower 304 stainless steel disk specimen by a carriage. The ball specimen was kept stationary during the test, whereas the disk specimen was driven with a constant rotating speed. The tests were performed under dry friction condition. Additional detailed information on the setup can be found in our previous works [35, 36].

In the tests, the applied nominal load was 49 N, and the diameter of the rotating sliding was 80 mm. The rotating speeds were set to 1, 4, 10, 15, and 30 rpm, corresponding to sliding velocities of 4.2, 16.75, 41.8, 62.8, and 125.6 mm/s, respectively. Loads of 19.6, 29.4, 39.2, 49, 58.8, 68.6, 78.4, and 88.2 N were applied to investigate the load effect at the same sliding velocity of 16.75 mm/s. The duration of each test was 3 min. All the tests were repeated several times to verify the repeatability of the experiments. New ball and disk specimens were used for different test conditions. The frictional force was measured every 0.01 s during the tests.

2.2 Measurement Techniques and Procedures

A real-time sound pressure spectrum analysis system (CRY2120U, CRY Sound Co., Ltd, China) was used to collect frictional noise at a frequency of 32,000 Hz. The deformational displacements of the ceramic ball holder were measured using a noncontact laser Doppler vibrometer (LDV) (OFV-506, Polytec GmbH, Germany) with 30,000 Hz. The laser beam was perpendicular to the holder and parallel to the frictional direction, as depicted in Fig. 1. An AE measuring instrument (DS5-16B, Beijing Softland Times Scientific & Technology Co., Ltd, China) was used to collect the AE signals on the holder surface (Fig. 1).

3 Results

3.1 Typical Frictional Vibration and Noise Behaviors

The frictional force curve in Fig. 2a depicts a typical stick–slip behavior during the Si_3N_4 ceramic/metal friction process. Figure 2b demonstrates the detail of the frictional force curve within 1 s. The frictional force showed the obvious time dependence. The rubbing pairs were relatively static during the sticking process [37]. The frictional force dropped abruptly and fluctuated violently for approximately 0.1 s during the slipping process. Figure 2c exhibits that the fluctuation of the vibrational displacement of

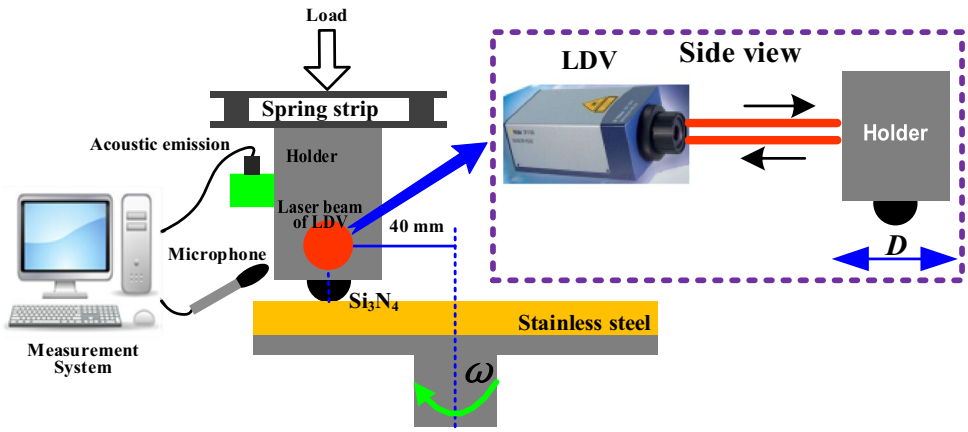

Fig. 1 Schematic of the test system used in this study

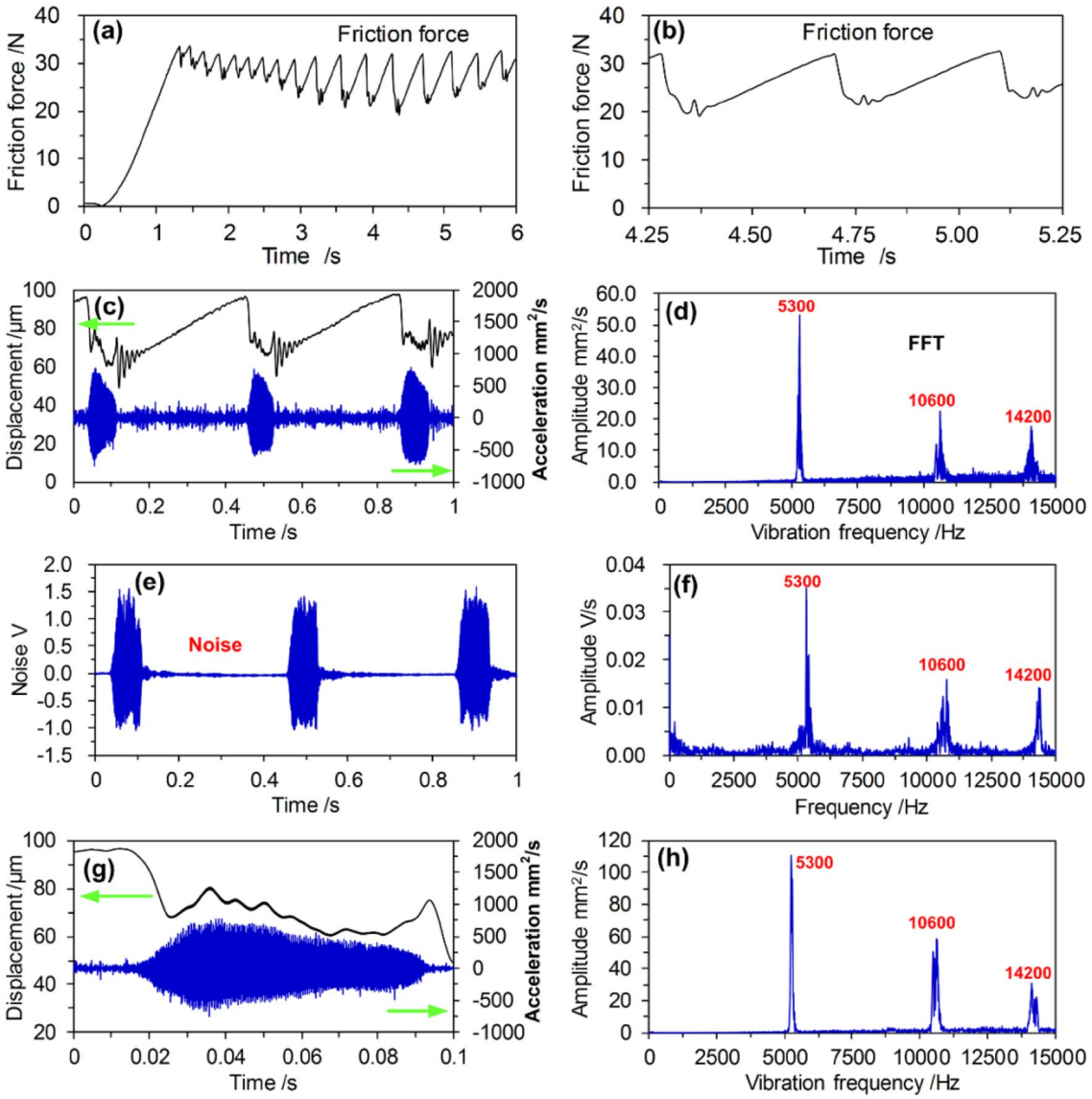

Fig. 2 Typical frictional vibration and noise during the stick–slip process between the Si_3N_4 ceramic/metal friction (49 N, 16.7 mm/s). **a** Typical stick–slip behavior; **b** detail of the frictional force curve within 1 s; **c** vibrational displacement and acceleration and **d** their frequency-domain spectrum of the ceramic ball holder during stick–slip process; **e** frictional noise and **f** its frequency-domain spectrum; **g** details of the vibrational displacement and acceleration and **h** their frequency-domain spectrum

the ceramic ball holder was consistent with the frictional force curve displayed in Fig. 2b. The frictional forces were obtained by measuring the deformational displacements of the ceramic ball holder along the sliding direction and were proportional to the displacements. The collection frequency (30 kHz) was much higher in deformational displacements than in frictional force (100 Hz). The deformational displacements of the ball holder were presented in the frictional force curve to characterize the stick–slip behavior in the subsequent sections. Figure 2c illustrates that the vibrational acceleration of the ceramic ball holder during the sticking process had a small wave, verifying the ball and disk were under a relatively static state. The vibrational acceleration changed sharply during the slipping process, indicating a relative movement occurred between the rubbing pairs. Its frequency-domain spectrum was achieved with a fast Fourier transform (FFT) analysis. The vibration mainly occurred at frequencies of approximately 5300, 10,600 (2 × 5300), and 14,000 Hz, as plotted in Fig. 2d, which presents a typical frequency doubling phenomenon. The frictional noise was radiated at the slipping stage, as depicted in Fig. 2e, and had excellent correspondence with the vibrational acceleration of the deformational displacement. Its main frequencies satisfied the major vibrational frequencies of the holder and

occurred at approximately 5300, 10,600, and 14,000 Hz. These test data directly disclosed that the frictional noise was radiated through severe frictional vibrations during the slipping processes. Thus, for convenience, the noise behaviors could be characterized by using the vibrational accelerations of the ceramic ball holder in the next sections. Figure 2g demonstrates the details of the displacement and vibrational acceleration in one stick–slip period. The displacement fluctuated frequently, although its amplitude was small at the initial stage during the slipping process. The vibrational acceleration increased gradually and lasted for nearly 0.07 s. The displacement fluctuations and their vibrational accelerations decreased gradually when the ceramic ball and steel disk contacted with each other again, and the vibrational accelerations presented a spindle-shaped change trend. Figure 2i exhibits that its major vibrational frequencies were consistent with the multiple vibrational accelerations displayed in Fig. 2d.

3.2 Influence of Speed on Frictional Vibration Behaviors During Stick–Slip Processes

Figure 3 displays the influence of speed on frictional vibration during the stick–slip process. The stick–slip periods and fluctuations were visible at low speeds, as presented in Fig. 3a, and were weakened as the increase in sliding speed (41.8 mm/s), as illustrated in Fig. 3c. These results were consistent with Dong's report [38]. The vibrational accelerations increased abruptly during the slipping process. All the severe vibration processes sustained approximately 0.07 s. However, the stick–slip periods and fluctuations were unclear at the high speed of 62.8 mm/s, as depicted in Fig. 3e. Frictional vibration also occurred during the sticking process. The vibrational acceleration presented a superposition phenomenon between two near-vibration waveforms. When the speed increased to 125.6 mm/s, the severe vibrations covered the whole sliding process, as demonstrated in Fig. 3g. The frequency-domain spectrum showed different characteristics as the increase in speed. At low speeds (4.2 and 41.8 mm/s), the vibrations mainly occurred at approximately 5300 Hz. With the increase in speed (62.8 mm/s), all vibrational frequencies were at approximately 5300, 10,600, and 14,000 Hz, higher than those at low speeds. At high speed (125.6 mm/s), the amplitude of vibration at 10,600 Hz was higher than that at approximately 5300 Hz. Moreover, the vibration at approximately 14,000 Hz was also evident, as exhibited in Fig. 3h, j. COFs at the end of tests and their fluctuating amplitudes increased as a function of velocity as shown in Fig. 3i and showed the same rule as major vibrational frequencies. High velocities worsened the wear process, and the frictional forces increased, which resulted in enhancing the vibrational displacements and their vibrational accelerations. In all, frictional vibration generally becomes apparent with the increase in speed, and the main vibrational frequency slowly shifts to a high frequency.

3.3 Influence of Load on Frictional Vibration Behaviors During Stick–Slip Processes

Figure 4 displays the influence of load on stick–slip and frictional vibration. Figure 4a, c, and e presents that the load had no significant effect on the stick–slip periods, but caused a considerable increase in the stick–slip fluctuations. A larger load not only enhanced the vibrational displacement of the ceramic ball holder, but also increased the vibrational acceleration, as illustrated in Fig. 4a, c, and e. Consequently, the amplitudes of all major vibrational frequencies at 5300, 10,600, and 14,000 Hz also increased, as depicted in Fig. 4b, d, f, and h. Because the COF was the ratio between frictional force and load, COF behaviors under different loads showed the similar behavior as shown in Fig. 4g. It is difficult to establish the relationships between the COF behaviors at the end of tests and vibrations.

4 Discussion

4.1 Mechanism of Frictional Vibration and Noise Generation

An excitation hammer was used to impact the ceramic ball holder and thus excited the natural vibration modes of the friction system. The vibrational displacement was measured using the LDV. The natural vibration frequencies, when the ceramic ball did not contact with the disk, were approximately 1800, 2700, 5150, 9000, and 12,600 Hz, as plotted in Fig. 5a. When the ceramic ball contacted with the disk at a load of 60 N, the holder was also impacted by the incentive hammer (the hammering point was close to the contact surface). The vibrational displacement, acceleration, and frequency-domain spectrum were measured, as demonstrated in Fig. 5b, c. The vibrational noise was generated when the ceramic ball holder was at the maximum deformation, as exhibited in Fig. 5b. The noise lasted at approximately 0.003 s. The vibrational frequency was at 5200 Hz, and close to the natural vibration frequency of the holder (5150 Hz). This value was also consistent with the frictional vibration frequency of 5300 Hz during slipping processes, as displayed in Figs. 2, 3, and 4. These phenomena were consistent with Mottershead's and Rhee's works [39, 40].

4.2 Mechanisms of Frictional Vibration

Fractures, deformations, scratches, and other behaviors of materials would occur during the contact shearing and impacts in wear processes and induced several types of

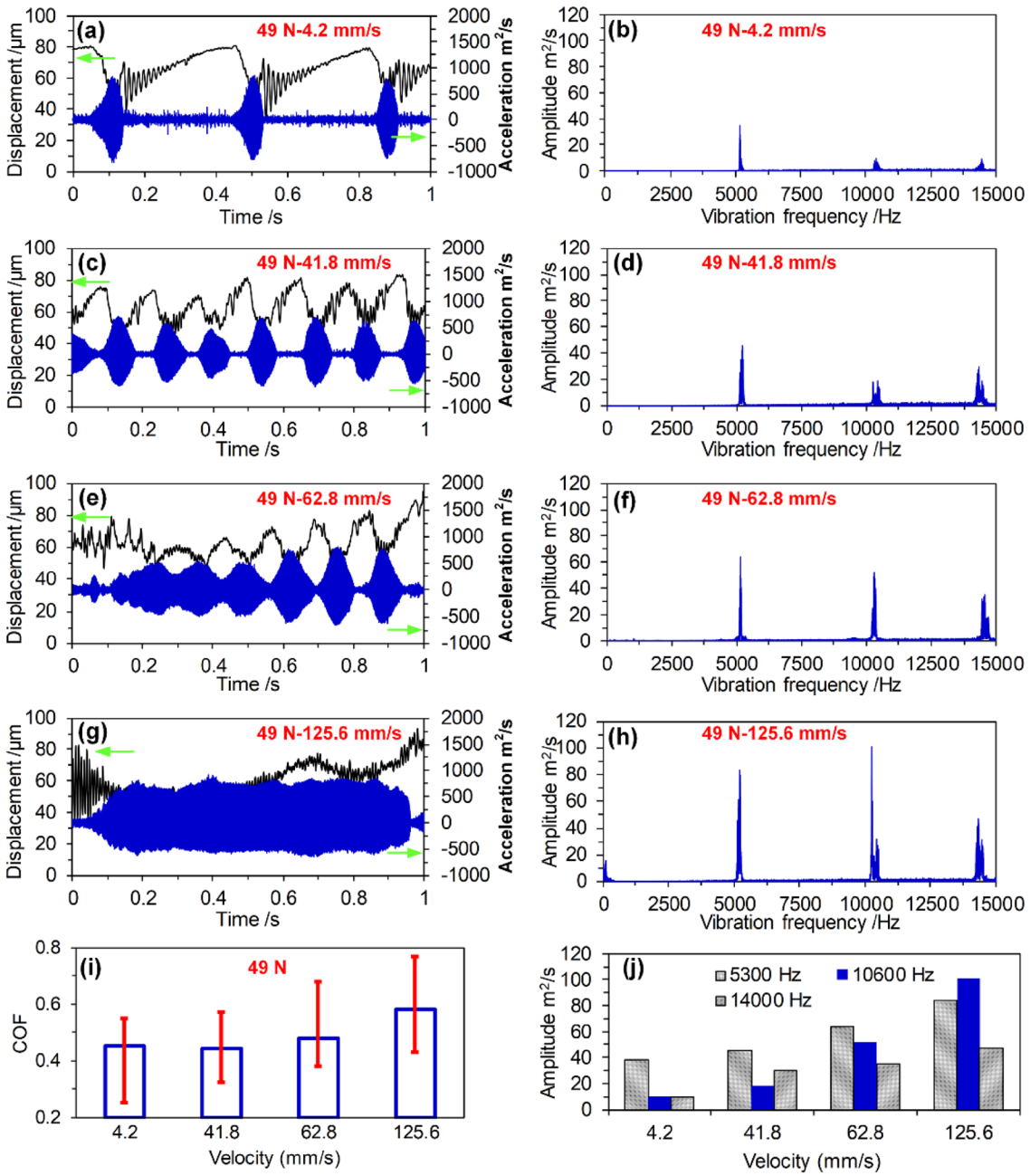

Fig. 3 Influence of speed on stick–slip and frictional vibration behaviors (dry friction and 49 N). **a** Vibrational displacement and acceleration and **b** their frequency-domain spectrum at 4.2 mm/s; **c** vibrational displacement and acceleration and **d** their frequency-domain spectrum at 41.8 mm/s; **e** vibrational displacement and acceleration and **f** their frequency-domain spectrum at 62.8 mm/s; **g** vibrational displacement and acceleration and **h** their frequency-domain spectrum at 125.6 mm/s; **i** COF behaviors at the end of tests under different velocities; **j** amplitudes of the major vibrational frequencies at different velocities

elastic waves, which resulted in AE [41–43], as presented in Fig. 6. Therefore, AE events could be used to represent the shearing or impacting conditions between the rough peaks on rubbing interfaces. Figure 7 illustrates the AE events and their number under different loads during the stick–slip process. Figure 7a depicts a typical AE event between the ball and disk during the slipping process with typical frequencies from 100,000 to 500,000 Hz (Fig. 7b). This AE event lasted about 0.0002 s [44]. The entire AE event set during a frictional vibration process is demonstrated in Fig. 7c. The event exhibited a spindle shape, which started at the initial stage of the slipping process and ended at the initial stage of the sticking process. It was consistent with the vibrational acceleration curve in

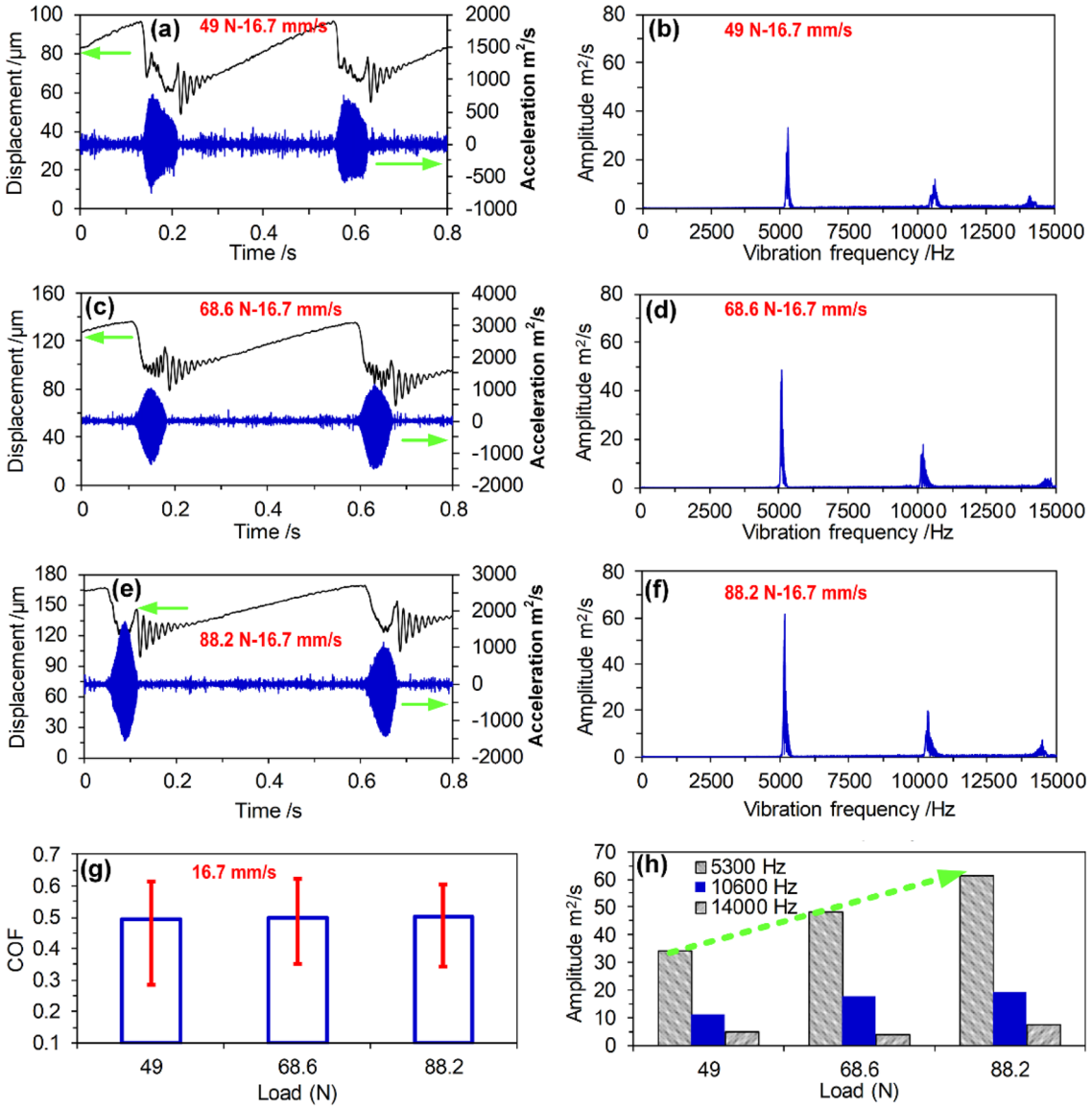

Fig. 4 Influence of load on stick–slip and frictional vibration behaviors (dry friction and 16.7 mm/s). **a** Vibrational displacement and acceleration and **b** their frequency-domain spectrum at 49 N; **c** vibrational displacement and acceleration and **d** their frequency-domain spectrum at 68.6 N; **e** vibrational displacement and acceleration and **f** their frequency-domain spectrum at 88.2 N; **g** COF behaviors at the end of tests under different loads; **h** amplitudes of the main vibrational frequencies at different loads

Fig. 2c. The AE event presented that contact shearing or impacting actions occurred during the slipping process, but not during the sticking process. Its main frequencies were in the range of 100,000–500,000 Hz, as exhibited in Fig. 7d. Every shearing or impacting action could force a ceramic ball holder to deform and vibrate [45]. The AE events were rapid and short but could be clearly calculated, as presented in Fig. 7e. These phenomena showed that the rough peaks on the disk wear surface sheared or impacted the rough peaks on the ceramic ball wear surface shortly and hurriedly. Figure 7f displays the number of AE events during the slipping processes under different loads, approximately 5500 per second, close to the main frequency of frictional vibrational acceleration (approximately 5300 Hz). The number of shearing and impacting actions was nearly equal to the forced vibrational frequency. When the number was close to a natural frequency of the frictional system, the frictional vibration and noise were enhanced, as described in Subsection 4.1. Frictional vibration may be attributed to the shearing or impacting actions of a rough contact between friction pairs during a slipping process [46].

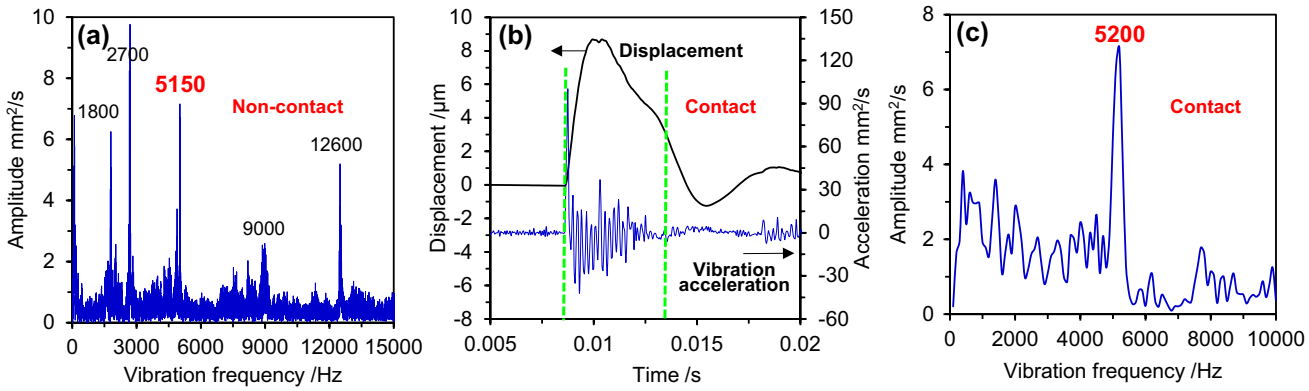

Fig. 5 Vibrational frequencies when an excitation hammer impacted the ceramic ball holder. **a** Natural frequencies of the ceramic ball holder when the ceramic ball did not contact with the disk; **b** vibrational displacement, acceleration, and **c** frequency-domain spectrum of the holder when the ceramic ball contacted with the disk

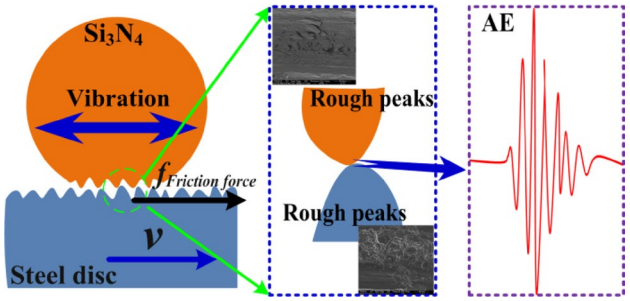

Fig. 6 Contact shearing or impacting actions between small rough peaks

4.3 Discussion on the Frequency-Multiplying Phenomenon of Frictional Vibration

Frictional vibration also occurred at 10,600 (2 × 5300 Hz) and 14,100 Hz. The typical vibrational displacement and acceleration during the slipping process are illustrated in Fig. 8a. Figure 8c, e, and g plots the generation, development, and decay stages of the frictional vibration, correspondingly. In the generation stage, the vibration displacement increased gradually and therefore also increased the vibration acceleration gradually. The main vibrational frequencies at 5300 and 10,600 were at high amplitudes, as depicted in Fig. 8d. When the frictional vibration developed further, the fluctuation amplitude of the vibrational displacement and acceleration increased and became larger than that in the generation stage. However, the main vibrational frequencies were comparatively singleness (Fig. 8f), and the vibration at approximately 5300 Hz was markedly enhanced, whereas the vibrations at approximately 10,600 and 14,200 Hz were considerably weakened. In the decay stage, the main vibrations presented diversification. In addition to the 5300 Hz, the vibration at frequency of 10,600 Hz evidently increased again as shown in Fig. 8h.

Figure 9a plots a superposition process of two adjacent frictional vibration waveforms to disclose frequency-multiplying phenomenon of the frictional vibration. The frictional vibrations occurred at frequencies of 5300 and 10,600 Hz, although the amplitude at 10,600 Hz was non-significant. The frictional vibrations of the front waveform and post-waveform (Fig. 9c, g) mainly occurred at 5300 Hz, as demonstrated in Fig. 9d, h. However, when the first vibration waveform in the decay stage met the second frictional vibration waveform in the generation stage, a superposition effect occurred. When the phases of two frictional vibration waveforms were different, they affected each other, as exhibited in Fig. 9e [47, 48]. Two vibrational waveforms were reinforcing slightly, and the vibration at 10,600 Hz was enhanced considerably, as displayed in Fig. 9f. This formed the frequency-multiplying phenomenon. The superposition phenomena between the two adjacent frictional vibrations could explain the frequency-multiplying phenomenon and the reinforcements of the high vibrational frequencies under the high velocities as presented in Fig. 3f, g.

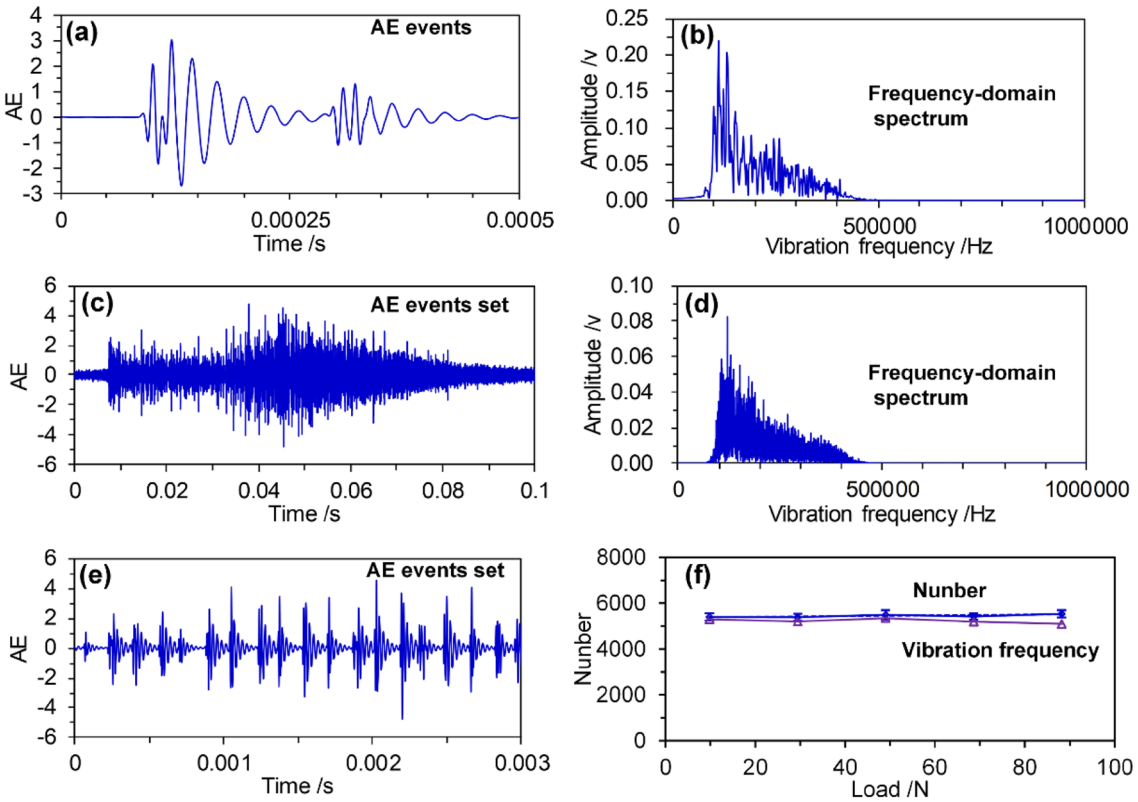

Fig. 7 AE events and their numbers under different loads during the stick–slip process. **a** Typical AE event between the ball and the disk and **b** its frequency-domain spectrum; **c** entire AE event set and **d** their frequency-domain spectrum during a complete frictional vibration process; **e** details of the AE events during the slipping process; **f** number of AE events and the main frequency during the slipping process under different loads

5 Conclusions

Frictional vibration and noise during a stick–slip process between Si_3N_4 ceramic/metal were studied. The results showed that frictional vibration and noise occur during the slipping process. In this process, the AE signals were obtained to confirm whether shearing or impacting actions between rough peaks on the rubbing pairs satisfy the main vibrational frequency of the frictional vibration acceleration. Thus, frictional vibration and noise might be attributed to the shearing or impacting action of a rough contact between the frictional pairs during the slipping process. A forced vibrational frequency is equal to the number of shearing or impacting actions. The main vibrational frequency rose slowly to a high frequency with the increase in speed. The vibrational accelerations and their main vibrational frequency increased with the increase in load. The superposition of frictional vibrations caused the multiplication of the frequency and the increase in the noise frequency shift.

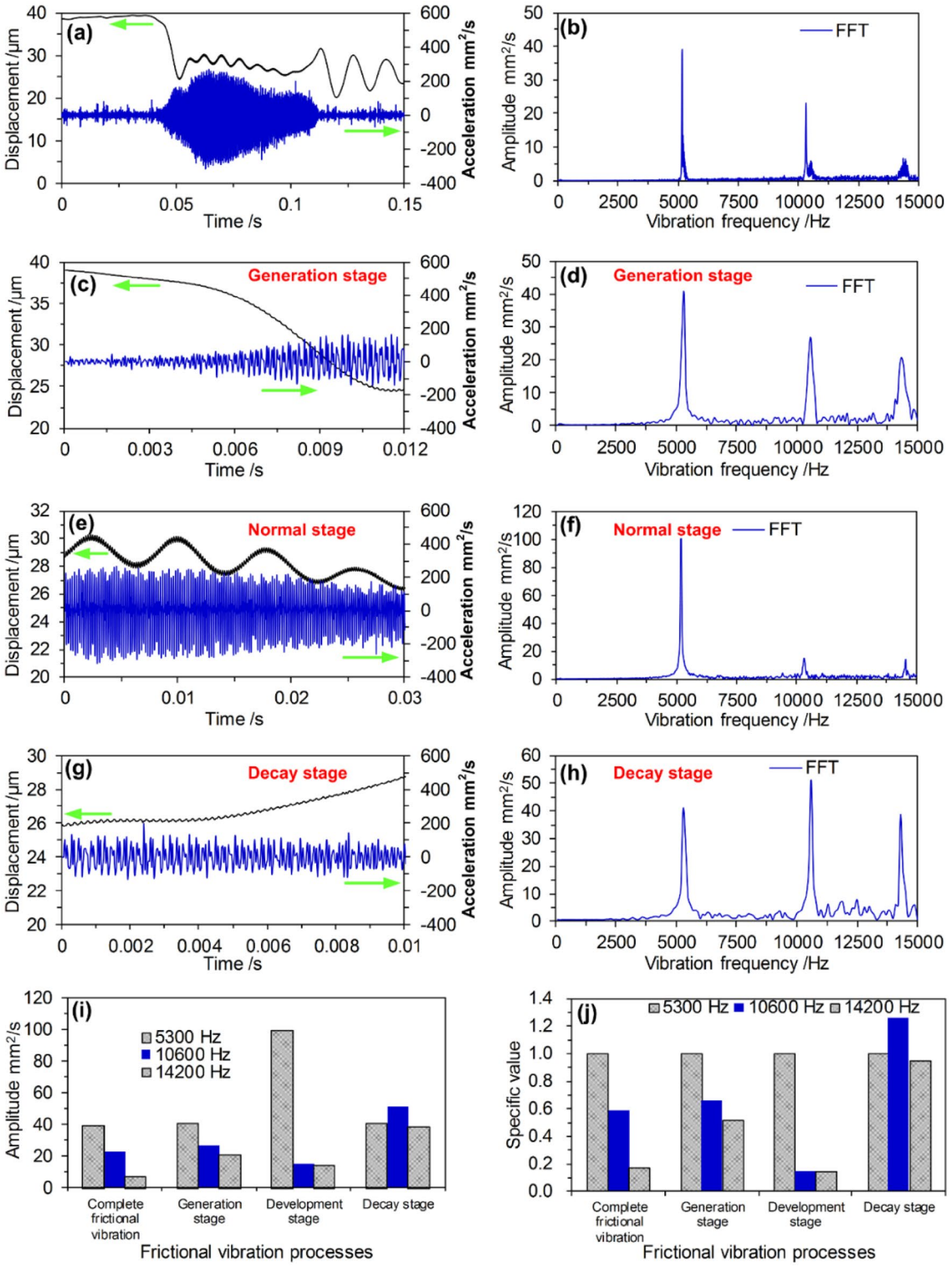

Fig. 8 Typical frictional vibration processes. **a** Vibrational displacement, acceleration, and **b** frequency-domain spectrum of a complete frictional vibration process; **c** vibrational displacement, acceleration, and **d** frequency-domain spectrum in the generation stage; **e** vibrational displacement, acceleration, and **f** frequency-domain spectrum in the development stage; **g** vibrational displacement, acceleration, and **h** frequency-domain spectrum in the decay stage; **i** amplitudes of the main vibrational frequencies at different stages; **j** specific value between the amplitudes of the main vibrational frequencies and the amplitude at 5300 Hz

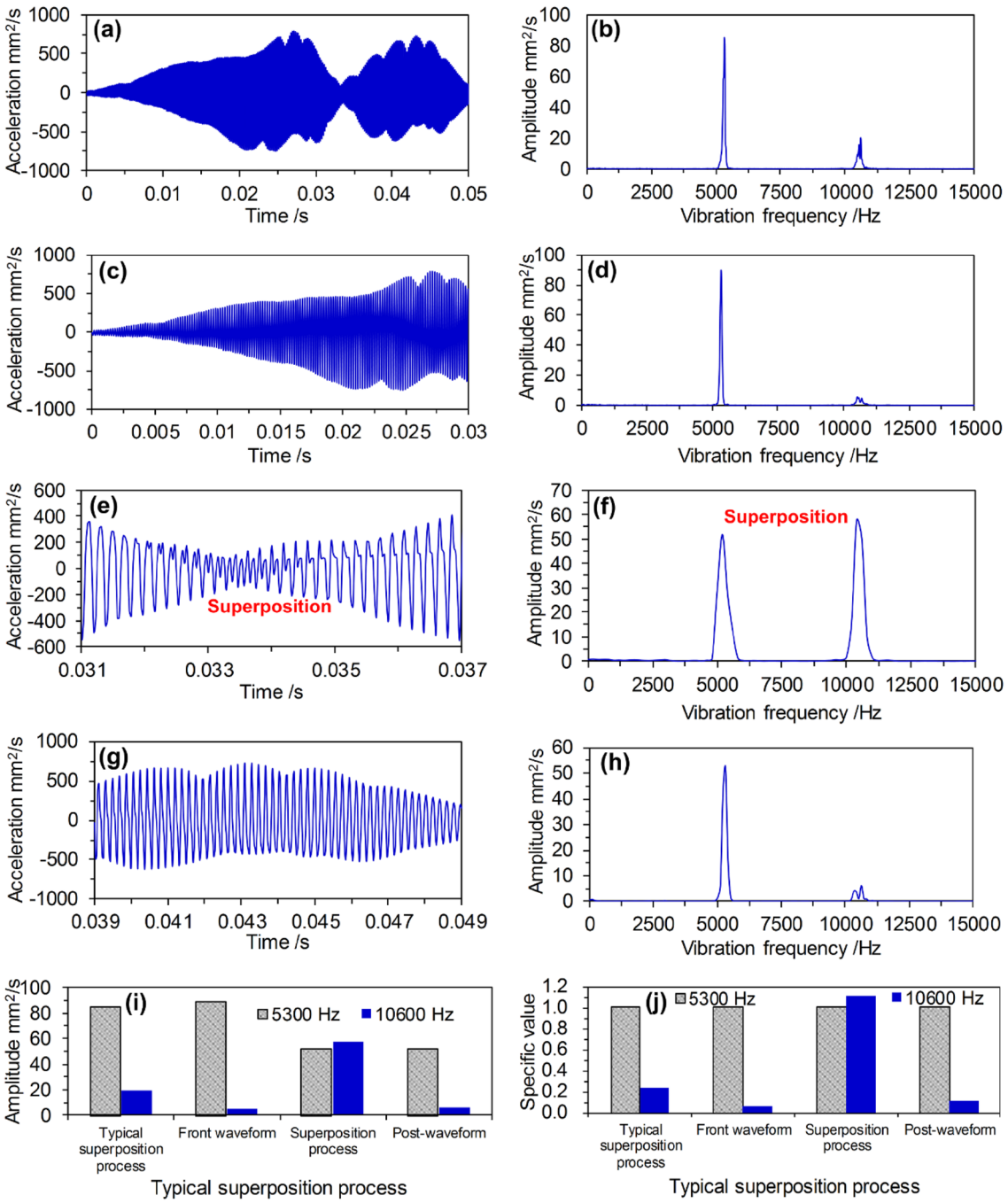

Fig. 9 Superposition processes of frictional vibration (49 N, 62.8 mm/s). **a** Typical superposition processes of two frictional vibration waveforms and **b** their frequency-domain spectrum; **c** front waveform and **d** its frequency-domain spectrum; **e** superposition process between two waveforms and **f** their frequency-domain spectrum; **g** post-waveform and **h** its frequency-domain spectrum; **i** amplitudes of the main vibrational frequencies at different processes; **j** specific value between the amplitudes of the main vibrational frequencies and the amplitude at 5300 Hz

Acknowledgements This study was supported by the National Natural Science Foundation of China (Grant Nos. 51605248, 51425502 and 51323006), the Hubei Provincial Natural Science Foundation of China (2018CFB130), the Joint Fund of the Ministry of Education, the High-Tech Ship Research Project of Ministry of Industry and Information Technology (No. MIIT[2016]547), and the Fundamental Research Funds for the Central South Universities (WUT: 2018IVA056).

References

1. Kinkaid, N.M., O'Reilly, O.M., Papadopoulos, P.: Automotive disc brake squeal. J. Sound Vib. **267**(1), 105–166 (2003)
2. Rouzic, J.L., Bot, A.L., Perret, L.J.: Friction-induced vibration by Stribeck's law: application to wiper blade squeal noise. Tribol. Lett. **49**(3), 563–572 (2013)
3. Dong, C.L., Yuan, C.Q., Bai, X.Q., Yan, X.P., Peng, Z.X.: Tribological properties of aged nitrile butadiene rubber under dry sliding conditions. Wear **322–323**, 226–237 (2015)
4. Meziane, A., Baillet, L., Laulagnet, B.: Experimental and numerical investigation of friction-induced vibration of a beam-on-beam in contact with friction. Appl. Acoust. **71**(9), 843–853 (2010)
5. Dong, C.L., Yuan, C.Q., Bai, X.Q., Yan, X.P., Peng, Z.X.: Study on wear behavior and wear model of nitrile butadiene rubber under water lubricated conditions. RSC Adv. **4**, 19034–19042 (2014)
6. Papinniemi, A., Lai, J.C.S., Zhao, J.Y., Loader, L.: Brake squeal: a literature review. Appl. Acoust. **63**, 391–400 (2002)
7. Chen, F.: Automotive disk brake squeal: an overview. Int. J. Veh. Des. **51**(1/2), 39–72 (2009)
8. Svetlizky, I., Fineberg, J.: Classical shear cracks drive the onset of dry frictional motion. Nature **509**(7499), 205–208 (2014)
9. Soobbarayen, K., Besset, S., Sinou, J.J.: Noise and vibration for a self-excited mechanical system with friction. Appl. Acoust. **74**(10), 1191–1204 (2013)
10. Chen, G.X., Zhou, Z.R., Ouyang, H.: A finite element study on rail corrugation based on saturated creep force-induced self-excited vibration of a wheelset-rail system. J. Sound Vib. **329**, 4643–4655 (2010)
11. Dong, C.L., Shi, L.C., Li, L.Z., Bai, X.Q., Yuan, C.Q., Tian, Y.: Stick-slip behaviours of water lubrication polymer materials under low speed conditions. Tribol. Int. **106**, 55–61 (2017)
12. John, H.C., Devon, E.A., Douglas, W.V.: A proposed mechanism for squeaking of ceramic-on-ceramic hips. Wear **269**(11–12), 782–789 (2010)
13. Rubinstein, S.M., Cohen, G., Fineberg, J.: Detachment fronts and the onset of dynamic friction. Nature **430**(7003), 1005–1009 (2004)
14. Chen, G.X., Zhou, Z.R.: A self-excited vibration model based on special elastic vibration modes of friction systems and time delays between the normal and friction forces: a new mechanism for squealing noise. Wear **262**, 1123–1139 (2007)
15. Ouyang, H., Mottershead, J.E., Brookfield, D.J., James, S., Cartmell, M.P.: A methodology for the determination of dynamic instabilities in a car disc brake. Int. J. Veh. Des. **23**(3/4), 241–262 (2000)
16. Graf, M., Ostermeyer, G.P.: Friction-induced vibration and dynamic friction laws: instability at positive friction–velocity-characteristic. Tribol. Int. **92**, 255–258 (2015)
17. Alan, H., Hiroshi, M., Masaki, W.: Correlation between features of acoustic emission signals and mechanical wear mechanisms. Wear **292–293**, 144–150 (2012)
18. Dong, C.L., Yuan, C.Q., Bai, X.Q., Li, J., Qin, H.L., Yan, X.P.: Coupling mechanism between wear and corrosion processes of 304 stainless steel in hydrogen peroxide environments. Sci. Rep. (UK) **7**, 2327 (2017)
19. Brunel, J.F., Dufrenoy, P., Nait, M.: Transient models for curve squeal noise. J. Sound Vib. **293**, 758–765 (2006)
20. Fan, Y.B., Gu, F.S., Ball, A.: Modelling acoustic emissions generated by sliding friction. Wear **268**(5–6), 811–815 (2010)
21. Tian, P., Tao, D., Yin, W., Zhang, X., Meng, Y., Tian, Y.: Creep to inertia dominated stick-slip behavior in sliding friction modulated by tilted non-uniform loading. Sci. Rep. (UK) **6**, 33730 (2016)
22. Fineberg, J., Marder, M.: Instability in dynamic fracture. Phys. Rev. Lett. **313**(1), 1–108 (1998)
23. Ben, D.O., Rubinstein, S.M., Fineberg, J.: Slip-stick and the evolution of frictional strength. Nature **463**(7277), 76–79 (2010)
24. Dong, C.L., Yuan, C.Q., Bai, X.Q., Qin, H.L., Yan, X.P.: Investigating relationship between deformation behaviours and stick-slip phenomena of polymer material. Wear **376–377**, 1333–1338 (2017)
25. Scholz, C.H.: Earthquakes and friction laws. Nature **391**(6662), 37–42 (1998)
26. Tian, P., Tian, Y., Shan, L., Meng, Y., Zhang, X.: A correlation analysis method for analyzing tribological states using acoustic emission, frictional coefficient, and contact resistance signals. Friction **3**(1), 36–46 (2015)
27. Oberst, S., Lai, J.C.S.: Statistical analysis of brake squeal noise. J. Sound Vib. **330**(12), 2978–2994 (2011)
28. Dong, C.L., Yuan, C.Q., Bai, X.Q., Yang, Y., Yan, X.P.: Study on wear behaviours for NBR/stainless steel under sand water-lubricated conditions. Wear **332–333**, 1012–1020 (2015)
29. Mo, J.L., Wang, Z.G., Chen, G.X., Shao, T.M., Zhu, M.H., Zhou, Z.R.: The effect of groove-textured surface on friction and wear and friction-induced vibration and noise. Wear **301**(1–2), 671–681 (2013)
30. Dong, C.L., Yuan, C.Q., Wang, L., Liu, W., Bai, X.Q., Yan, X.P.: Tribological properties of water-lubricated rubber materials after modification by MoS_2 nanoparticles. Sci. Rep. (UK) **6**, 35023 (2016)
31. Livne, A., Bouchbinder, E., Svetlizky, I.: The near-tip fields of fast cracks. Science **327**(5971), 1359–1363 (2010)
32. Popp, K., Rudolph, M.: Vibration control to avoid stick-slip motion. J. Vib. Control **10**(11), 1585–1600 (2004)
33. Charles, K.C., Ahmed, E.E., Langer, J.S., Carlson, J.M.: Stick-slip instabilities in sheared granular flow: the role of friction and acoustic vibrations. Phys. Rev. E **92**, 022209 (2015)
34. Johnson, P.A., Ferdowsi, B., Kaproth, B.M., et al.: Acoustic emission and microslip precursors to stick-slip failure in sheared granular material. Geophys. Res. Lett. **40**(21), 5627–5631 (2013)
35. Zhou, X., Mo, J.L., Li, Y.Y., Xu, J.Y., Zhang, X., Cai, S., Jin, Z.M.: Correlation between tactile perception and tribological and dynamical properties for human finger under different sliding speeds. Tribol. Int. **123**, 286–295 (2018)
36. Wang, D.W., Mo, J.L., Wang, Z.G., Chen, G.X., Ouyang, H., Zhou, Z.R.: Numerical study of friction-induced vibration and noise on groove-textured surface. Tribol. Int. **64**, 1–7 (2013)
37. Viswanathan, K., Sundaram, N.K., Chandrasekar, S.: Stick–slip at soft adhesive interfaces mediated by slow frictional waves. Soft Matter **12**(24), 5265 (2016)
38. Dong, C.L., Yuan, C.Q., Xu, A., Bai, X.Q., Tian, Y.: Rippled polymer surface generated by stick–slip friction. Langmuir **35**(7), 2878–2884 (2019)
39. Mottershead, J.E.: Vibrations and friction-induced instability in discs. Shock Vib. Digest **30**(1), 14–31 (1998)
40. Rhee, S.K., Tsang, P.H.S., Wang, Y.S.: Friction-induced noise and vibration of disc brakes. Wear **133**(1), 39–45 (1989)

41. Johnson, A., Ferdowsi, B., Kaproth, B.M., et al.: Acoustic emission and microslip precursors to stick-slip failure in sheared granular material. Geophys. Res. Lett. **40**(21), 5627–5631 (2013)
42. Bot, A.L., Chakra, E.B.: Measurement of friction noise versus contact area of rough surfaces weakly loaded. Tribol. Lett. **37**(2), 273–281 (2010)
43. Soobbarayen, K., Besset, S., Sinou, J.J.: A simplified approach for the calculation of acoustic emission in the case of friction-induced noise and vibration. Mech. Syst. Signal Pr. **50–51**, 732–756 (2015)
44. Droubi, M.G., Reuben, R.L., Steel, J.A.: Flow noise identification using acoustic emission (AE) energy decomposition for sand monitoring in flow pipeline. Appl. Acoust. **113**, 5–15 (2017)
45. Duc, N.D., Tuan, N.D., Tran, P., et al.: Nonlinear dynamic response and vibration of imperfect shear deformable functionally graded plates subjected to blast and thermal loads. Mech. Compos. Mater. Struct. **24**(4), 12 (2017)
46. Toh, C.K.: Vibration analysis in high speed rough and finish milling hardened steel. J. Sound Vib. **278**(1–2), 101–115 (2004)
47. Lee, K.Y., Huang, C.F., Huang, K.N., et al.: Two-frequency ultrasonic system with direct digital frequency synthesizers and vernier caliper phase meter for measuring air temperature. Sens. Mater. **24**(7), 397–412 (2012)
48. Trapero, J.R., Hebertt, S.R., Batlle, V.F.: An algebraic frequency estimator for a biased and noisy sinusoidal signal. Signal Process. **87**(6), 1188–1201 (2007)